





C-band 100-GBaud PS-PAM-4 transmission over 50-km SSMF enabled by FIR-filter-based pre-electronic dispersion compensation

XIONG WU,¹  JUNWEI ZHANG,^{1,2,*}  ALAN PAK TAO LAU,^{3,4} AND CHAO LU^{1,2,4}

¹Photonics Research Institute, Department of Electronic and Information Engineering, The Hong Kong Polytechnic University, Hong Kong, China

²State Key Laboratory of Optoelectronic Materials and Technologies, School of Electronics and Information Technology, Sun Yat-Sen University, Guangzhou 510275, China

³Photonics Research Institute, Department of Electrical Engineering, The Hong Kong Polytechnic University, Hong Kong, China

⁴The Hong Kong Polytechnic University Shenzhen Research Institute, Shenzhen 518057, China

*jun-wei.zhang@polyu.edu.hk

Abstract: Chromatic dispersion (CD) is always an obstacle to C-band high-speed intensity modulation and direct detection (IM/DD) transmissions, especially with a fiber reach of > 20 km. To reach beyond net-100-Gb/s IM/DD transmission over 50-km standard single mode fiber (SSMF), we for the first time present a CD-aware probabilistically shaped four-ary pulse amplitude modulation (PS-PAM-4) signal transmission scheme with a FIR-filter-based pre-electronic dispersion compensation (FIR-EDC) for C-band IM/DD transmission system. With the help of the FIR-EDC at the transmitter, 100-GBaud PS-PAM-4 signal transmission at 150-Gb/s line rate and 115.2-Gb/s net rate over 50-km SSMF is realized with only feed-forward equalization (FFE) at the receiver side. The superiority of the CD-aware PS-PAM-4 signal transmission scheme over other benchmark schemes has been successfully verified by experiments. Experimental results show that 24.5% improvement of system capacity is obtained by the FIR-EDC-based PS-PAM-4 signal transmission scheme in comparison to the FIR-EDC-based on-off keying (OOK) signal transmission scheme. Compared with the FIR-EDC-based uniform PAM-4 signal transmission scheme or the PS-PAM-4 signal transmission scheme without EDC, the capacity improvement obtained by the FIR-EDC-based PS-PAM-4 signal transmission scheme becomes more profound. The results show the potential and feasibility of such CD-aware PS-PAM-4 signal transmission scheme applied in CD-constrained IM/DD datacenter interconnects.

© 2023 Optica Publishing Group under the terms of the [Optica Open Access Publishing Agreement](#)

1. Introduction

Propelled by the rapid traffic growth of bandwidth-consuming services like video streaming, cloud computing, and virtual/mixed reality, the development of high-speed datacenter interconnects and access networks has attracted much attention in recent years. To support higher throughput demand for these short-reach communication scenarios, intensity modulation and direct detection (IM/DD) scheme with spectrally efficient modulations is regarded as the most viable and cost-effective option owing to its low cost, high energy-efficiency, and small form factors [1,2]. Among different modulation schemes, M -ary pulse amplitude modulation (PAM- M) is preferred owing to the balance between performance and complexity [1,2]. Benefiting from significant shaping gain or increasing information rate over the uniform PAM signal, rate-adaptable probabilistically shaped PAM (PS-PAM) signal has been extensively applied in IM/DD transmission links with fiber lengths up to 2 km [3–6] and 20 km [7,8] in the C band and O band, respectively.

With longer transmission distances of > 20 km in the C band, the achievable data rates/ baud rates of PAM-based IM/DD systems are mainly limited by chromatic dispersion (CD) [9–21]. Due to the interaction of CD and square-law detection, the resulted frequency selective power fading leads to spectral zeros inside the signal spectrum and degrades the transmission performance. This impairment becomes severer with a higher baud rate and/or a longer fiber reach. To combat CD-induced power fading, digital signal processing (DSP) is a promising candidate without the need to employ costly optoelectronics. The receiver-side decision-feedback equalizer (DFE) [9], receiver-side weighted DFE (WDFE) [10], transmitter-side Tomlinson-Harashima precoding (THP) [9], and their improved counterparts like Volterra DFE (VDFE) [11,12] and nonlinear WDFE/THP [13,14] with an infinite impulse response (IIR) structure can efficiently equalize the CD-induced spectral zeros by pole insertion. However, these equalizers require at least dozens of feedback taps to reach desired transmission performance, which prohibits their real-time hardware implementation and limits the circuit throughput [15]. Moreover, the rate-adaptable PS-PAM signal is incompatible with the DFEs or THPs, which would cause significant distortion of the log-likelihood ratio (LLR) distribution and thus degrade the mutual information (MI) [22].

Recently, transmitter-side iterative pre-electronic dispersion compensation (EDC) algorithms were presented [16–19] and experimentally demonstrated for on-off keying (OOK)/PAM-based IM/DD systems over standard single-mode fibers (SSMFs) with distances beyond 40 km [17–19]. These EDC algorithms are based on Gerchberg-Saxton (GS) in an iterative manner (GS-EDC for short). Generally, at each iteration GS-EDC adds phase and amplitude constraints on all the transmitted signals at the digital transmitter and receiver, respectively. The dynamic real-time iterations result in high computational complexity and increase the power consumption of the DSP module. To solve this problem, a novel non-iterative finite-impulse-response-filter-based pre-EDC (FIR-EDC) scheme simplified with the GS algorithm has been proposed [20,21] and experimentally demonstrated in a 56-Gb/s OOK transmission system over 80-km SSMF [21]. Nonetheless, the achievable data rates of these non-iterative pre-EDC IM/DD demonstrations using the conventional OOK/PAM signal are still lower than 100 Gb/s, which could be further improved. Besides, high-speed PS-PAM signal transmission over > 20 km dispersion-uncompensated link has not been reported yet. Adopting rate-adaptable PS-PAM- M signal over longer fiber reach (e.g., ER and beyond ER [15,23]) is meaningful for high-speed IM/DD datacenter interconnects.

In this paper, we for the first time present and experimentally demonstrate a CD-aware PS-PAM-4 signal transmission scheme to combat the CD-induced impairments and maximize the capacity for C-band IM/DD system. By performing a non-iterative FIR-EDC at the transmitter, only feed-forward equalization (FFE) is required to adaptively equalize the residual linear inter-symbol interference (ISI) at the receiver, greatly simplifying the DSP implementation. Signal transmissions at 100 GBaud over 50-km SSMF have been conducted to evaluate the performance of the proposed rate-adaptable PS-PAM-4 signal transmission scheme with FIR-EDC and further compared with other transmission schemes using uniform PAM-4/OOK signal with FIR-EDC and PS-PAM-4 signal without EDC, verifying the superiority of the CD-aware PS-PAM-4 signal transmission scheme. To the best of our knowledge, we demonstrate the first C-band net-115.2-Gb/s and line-150-Gb/s CD-aware PS-PAM-4 IM/DD transmission over 50 km dispersion-uncompensated link.

2. Principle of FIR-EDC

Unlike the iterative pre-EDCs involving signal processing at each iteration, cost-effective FIR-EDC only updates the weights of all taps in an iterative manner, regardless of the signal itself. Thus, the FIR-EDC can be regarded as a non-iterative EDC in the signal angle. Once the CD coefficient is obtained, the weights of FIR-EDC can be calculated and stored before performing on the transmitted IM/DD signal and is transparent to the signal and format.

The principle is illustrated below. t_s is the index of samples/taps of FIR-EDC when operating at two samples per symbol (sps). The unit impulse response (i.e., the weights of 1 at the central tap and 0 at other taps, $[0, \dots, 0, 1, 0, \dots, 0]$) is posed with a pre-defined digital extinction ratio (DER) $10\log_{10}\frac{b}{a}|_{a,b>0}$, and it turns to $[a, \dots, a, b, a, \dots, a]$. Next, $h_{\text{FIR}}^{(n)}(t_s)$ is initialized to $\sqrt{[a, \dots, a, b, a, \dots, a]}$. At n^{th} iteration, $h_{\text{FIR}}^{(n)}(t_s)$ is updated only in its amplitude and its phase is removed. Then it is sent to digitally-forward-transmission over SSMF with the CD coefficient of $+D$. At the digital receiver, the received response $h_r^{(n)}(t_s)$ is obtained, namely the convolution of $h_{\text{FIR}}^{(n)}(t_s)$ and CD channel response $h_{+D}(t_s)$. The amplitude constraint is performed to $h_r^{(n)}(t_s)$ that its original amplitude is replaced with the transmitted initial response $h_{\text{FIR}}^{(0)}(t_s)$ and the phase $\angle h_r^{(n)}(t_s)$ remains. After that, the updated $h_r^{(n)}(t_s)$ at the digital receiver is transmitted backwardly to the digital transmitter, through the CD channel response $h_{-D}(t_s)$. Hence, the FIR filter at the transmitter is changed and only its amplitude is ready for the next iteration. After N iterations, the final pre-filter $h_{\text{Tx}}(t_s)$ by FIR-EDC is assigned to $|h_{\text{FIR}}^{(N)}(t_s)|^2$ with mean removal. Then the final transmitted signal with pre-compensation is the convolution of the original pulse-shaped signal $s(t_s)$ and $h_{\text{Tx}}(t_s)$. The pulse shaping filter can also be embedded in the FIR-EDC as the initial impulse response for iteration. It is worth mentioning that the GS-EDC has a similar procedure as FIR-EDC, but the former processes signal by replacing the input $h_{\text{FIR}}^{(n)}(t_s)$ of FIR-EDC with $\sqrt{s^{(n)}(t_s)}$, amplitude of all the transmitted pulse-shaped intensity signal $s^{(n)}(t_s)$, to update in each iteration. Consequently, the GS-EDC consumes much more operational complexity in real-time transmission.

Algorithm 1: FIR-EDC

Result: $h_{\text{Tx}}(t_s) = |h_{\text{FIR}}^{(N)}(t_s)|^2$ and $s_{\text{Tx}}(t_s) = s(t_s) * h_{\text{Tx}}(t_s)$.

Initialization: $h_{\text{FIR}}^{(0)}(t_s) = \sqrt{[a, \dots, a, b, a, \dots, a]}$.

for $n = 1 : N$ **do**

 Amplitude constraint at the digital transmitter:

$$h_{\text{FIR}}^{(n)}(t_s) = |h_{\text{FIR}}^{(n-1)}(t_s)|.$$

 SSMF forward transmission ($+D$):

$$h_r^{(n)}(t_s) = h_{\text{FIR}}^{(n)}(t_s) * h_{+D}(t_s) = |h_{\text{FIR}}^{(n)}(t_s)| e^{j\angle h_r^{(n)}(t_s)}.$$

 Amplitude constraint at the digital receiver:

$$h_r^{(n)}(t_s) = |h_{\text{FIR}}^{(0)}(t_s)| e^{j\angle h_r^{(n)}(t_s)}.$$

 SSMF backward transmission ($-D$):

$$h_{\text{FIR}}^{(n)}(t_s) = h_r^{(n)}(t_s) * h_{-D}(t_s).$$

end

3. Experimental setup and results

Normalized generalized mutual information (NGMI) is adopted here as a performance metric of transmissions with soft-decision forward error corrections (SD-FECs) [3,5,24,25] which can be expressed as:

$$\text{NGMI} = 1 - \frac{H - \text{GMI}}{\log_2(M)}, \quad (1)$$

where H and M are the entropy and the PAM order, respectively, and the GMI is estimated by the bit-wise LLR [26].

In addition, a concatenated FEC with a total code rate of 0.826 consisting of an inner low-density parity-check (LDPC) code with a code rate of 5/6 (64800, 54000) and an outer Bose-Chaudhuri-Hocquenghem (BCH) (30832, 30592) code is assumed to be used, and the threshold NGMI for this concatenated FEC is 0.857 [3,5,24]. Hence, the net rate of PS-PAM- M /PAM- M can be calculated as:

$$\text{Net rate} = [\text{Entropy} - (1 - 0.826) \times \log_2(M)] \times \text{Baud rate}, \quad (2)$$

where the PS-PAM- M signals with different entropies are generated by varying the shaping factor of the Maxwell-Boltzmann (MB) distribution using a constant composition distribution matcher (CCDM) [24,27], and the entropy of conventional PAM- M is always equal to $\log_2(M)$. Specifically for PS-PAM-4 signal, the probabilities of its four levels ($-3, -1, +1, +3$) and its achieved net rates at 100 GBaud are depicted in Fig. 1, changed by different entropies (from 1.1 to 1.8 at intervals of 0.1). Understandably, the increase of entropy, namely the data rate, results in the increases of probabilities of the outer levels of PS-PAM-4 signal, which are close to those of inner levels, namely approaching PAM-4 from OOK. Note that these entropies will also be adopted in the following experiments.

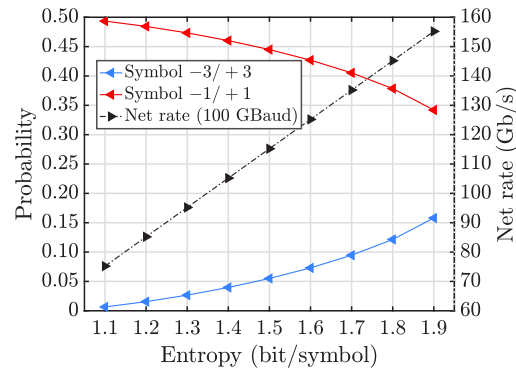


Fig. 1. Probability (left y-axis) and net rate (right y-axis) as a function of entropy for 100-GBaud PS-PAM-4 signal.

The performance of the proposed CD-aware PS-PAM-4 signal transmission scheme is evaluated in a C-band IM/DD system over 50-km SSMF, as the experimental setup and DSP block diagram shown in Fig. 2(a), where inserts (I) and (II) give the transmission curve of the used Mach-Zehnder modulator (MZM) and the overall electrical response of the experimental setup for the back-to-back (B2B) link, respectively. At the transmitter, the 100-GBaud PS-PAM-4 signal is generated offline and pulse shaped sequentially with 0.1 roll-off-factor (RoF) raised-cosine (RC) pulse and FIR-EDC at 2 samples per symbol (sps). Then the PS-PAM-4 signal is resampled to 120-GSa/s and digital-to-analog converted by an arbitrary waveform generator (AWG, Keysight M8194A). After amplified by an electrical amplifier (EA), the resulting PS-PAM-4 signal drives the MZM to achieve the linear intensity modulation over the light beam from an external cavity laser (ECL) at 1550.12 nm. The optical spectra of the carrier and PS-PAM-4 signals at the transmitter are depicted in Fig. 2(b). Then the modulated light is sent to 50-km SSMF for transmission. At the receiver, before direct detection by a 70-GHz photodetector (PD), the received optical signal is boosted by an erbium-doped fiber amplifier (EDFA) with 7-dBm output power, and then a variable optical attenuator (VOA) is followed to change the received optical power (ROP) injected into PD to evaluate the system's power budget. Finally, the detected signal is recorded by 256-GSa/s oscilloscope (OSC, Keysight UXR0804A) and processed by digital signal processing (DSP) procedures of resampling, synchronization, simple FFE operated at 2-sps

mode, and final NGMI calculation. The electrical spectra of received PS-PAM-4 signals without and with FIR-EDC are shown in Figs. 2(b) and 2(c), respectively. Meanwhile, the theoretically calculated frequency power fading responses [17,28,29] are plotted for comparison. Obviously, the power fading effect is effectively mitigated after performing the FIR-EDC.

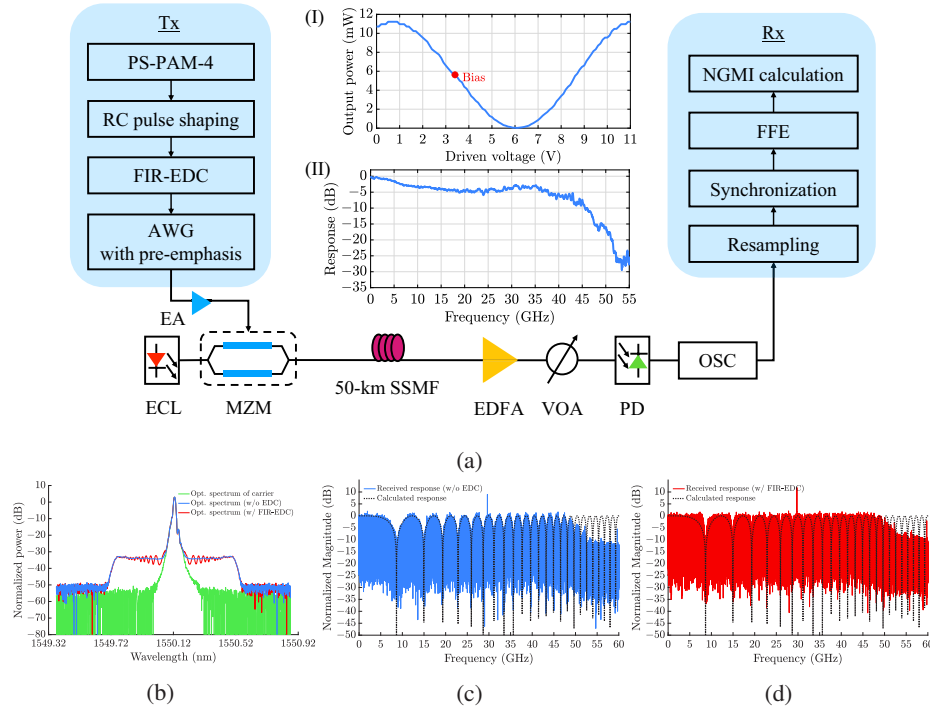


Fig. 2. (a) Experimental setup and DSP. (I) Transmission curve of MZM; (II) Overall electrical response under B2B link. (b) Optical spectra of carrier, and optical PS-PAM-4 signals without and with FIR-EDC, respectively. Received electrical responses of PS-PAM-4 signals (c) without EDC and (d) with FIR-EDC.

Fixed at 30 iterations for 100-GBaud PS-PAM-4 signal with an entropy of 1.5-bit/symbol, the impact of different numbers of FIR-EDC taps on NGMI is evaluated under various DERs. The corresponding results are presented in Fig. 3(a), applying with 111-tap T/2 FFE at the receiver for the residual ISI cancellation. It can be shown that the difference in DERs has little effect on NGMI, and more number of taps is beneficial to the improvement of NGMI in general. Specifically, 1101 FIR-EDC taps are enough to make the NGMI value meet the threshold of 0.857 and 1501 taps are almost optimal at 0.5-dB DER considering the NGMI performance and the complexity of FIR-EDC. These adopted values can also be found in Fig. 3(b) for 1.5-bit/symbol PS-PAM-4 signal with the DER set to 0.5 dB where the change of NGMI with the combination of FIR-EDC taps and FFE taps is detailed. As a result, 1501-tap FIR-EDC and 111-tap FFE are chosen for the following analysis to better explore the performance of CD-aware PS-PAM-4 signal transmission scheme. Admittedly, more cost-effective combinations can be found for the cases where the FFE has fewer number of taps along with 1101-tap FIR-EDC to meet the 0.875 NGMI threshold. Apparently, the normalized FIR-EDC with mean removal has a symmetrical weight distribution using different DERs, as shown in Fig. 4(a). Among these tested DERs, there is an ignorable difference in their resulting weight distributions, consistent with the similarity of results shown in Fig. 3(a). Notably, the complexity of FIR-EDC can be further reduced by the weight sharing/weight clustering strategy [11,30,31], in which the tap weights with similar values

can be grouped into a new weight and thus reducing the tap redundancy for FIR-EDC. What's more, the weights of FFE at the receiver are also presented in Fig. 4(b). It shows the major ISI is induced among adjacent few samples after using FIR-EDC, but non-negligible ISI still exists for a longer duration, which also explains the benefit of FFE with more number of taps.

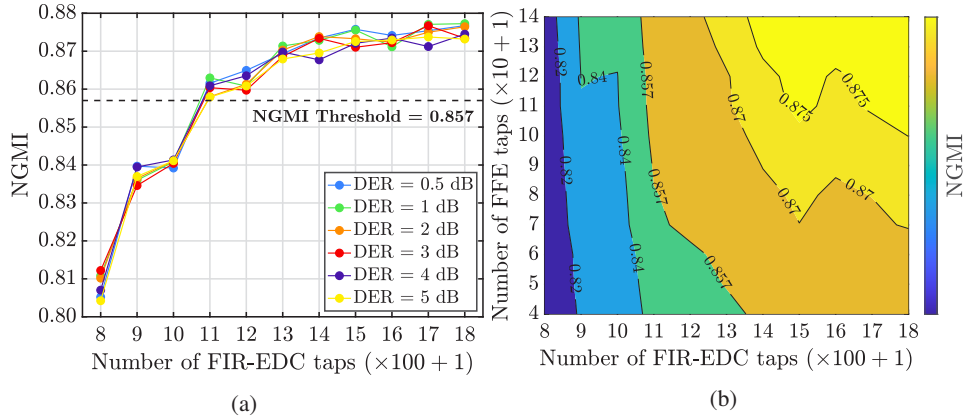


Fig. 3. (a) Impact of the number of FIR-EDC taps on NGMI under different DERs, using 111-tap FFE. (b) Impact of the number of FFE taps and the number of FIR-EDC taps on NGMI with a DER of 0.5 dB.

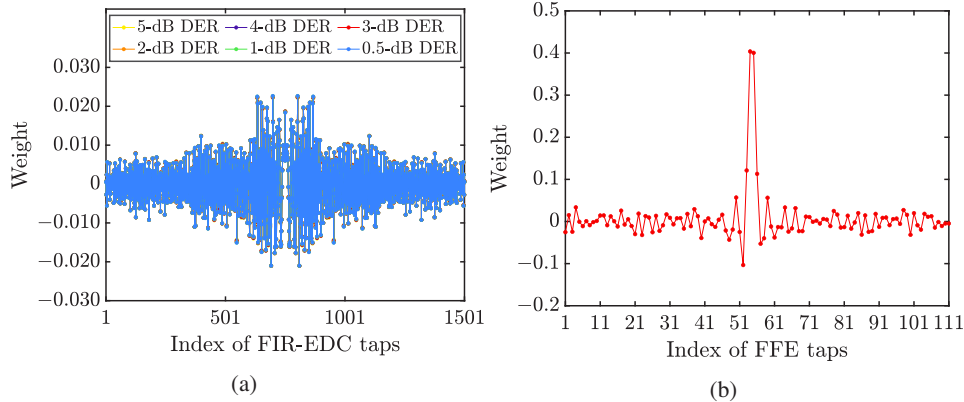


Fig. 4. (a) Weight distributions of FIR-EDC taps using different DERs. (b) Weight distribution of FFE taps.

To evaluate the superiority of CD-aware PS-PAM-4 signal transmission scheme, the uniform PAM-4 and OOK signals with different baud rates are compared, all pre-compensated with FIR-EDC with DER optimized separately. The baud rate of PS-PAM-4 signal is fixed at 100 GBaud and the entropy is changed from 1.1 to 1.8 at intervals of 0.1. The baud rate of OOK signal is changed from 100 GBaud to 120 GBaud at intervals of 4 GBaud, while the tested baud rates of PAM-4 signal are 50 GBaud and 100 GBaud. Detailed results are depicted in Fig. 5(a). It can be observed that the PAM-4 signal has the worst NGMI performance among all signals and is inoperable. The OOK signal is the optimal format only in a small range and degrades dramatically with increased baud rate/net rate due to the bandwidth limitation (see inset II in Fig. 2(a)). When the achieved net rate exceeds 90 Gb/s, the PS-PAM-4 signal is the optimal option among these three, and the NGMI penalty between the OOK and PS-PAM-4 signals

is also enlarged with the increase of net rate. With the NGMI above the threshold of 0.857, the achievable net rate (line rate) of the PS-PAM-4 signal is 115.2 Gb/s (150 Gb/s), which is improved by $\sim 24.5\%$ (i.e., 22.7-Gb/s increase in data rate) compared with net 92.5 Gb/s achieved by OOK signal. When compared with the uniform PAM-4 signal, the capacity improvement obtained by the PS-PAM-4 signal becomes more profound. Moreover, even for the PS-PAM-4 signal, the reachable entropy is less than 1.6 bit/symbol under the NGMI threshold of 0.857. Another comparison is conducted for 100-GBaud PS-PAM-4 signal with different net rates using different pre-EDC schemes, including the FIR-EDC, GS-EDC, and no pre-EDC, as the results presented in Fig. 5(b). It is seen that without any pre-EDC, the NGMI cannot reach the threshold of 0.857. Since the FIR-EDC only performs as linear pre-compensation, the GS-EDC involving nonlinearity during signal processing in each iteration has a particular improvement in NGMI regardless of data rate, which can also be observed from Fig. 5(b). The GS-EDC improves approximately 10 Gb/s in net rate compared to the FIR-EDC, but the iterative processing hinders its practicality. As a good trade-off, the FIR-EDC is promising in practice and is transparent to any format.

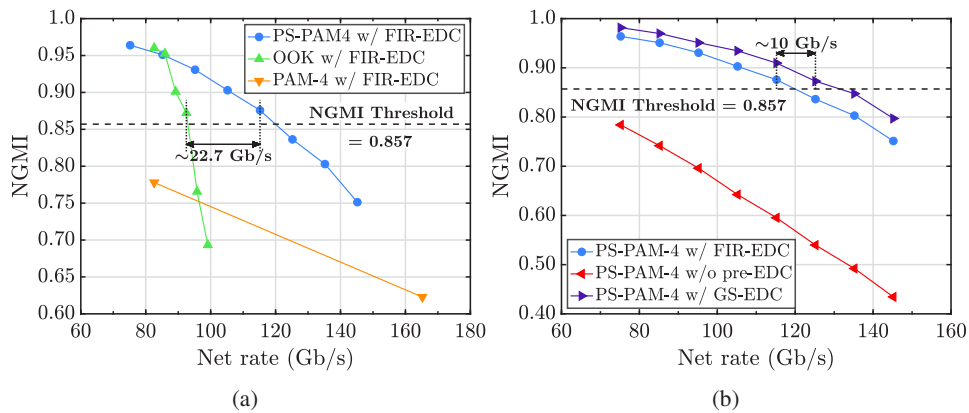


Fig. 5. (a) Achievable NGMI of PS-PAM-4, OOK, and PAM-4 signals with different net rates, using FIR-EDC. (b) Achievable NGMI of PS-PAM-4 signals with different net rates, using FIR-EDC, no pre-EDC, and GS-EDC.

Lastly, the required ROPs of two 100-GBaud PS-PAM-4 signals are measured using the FIR-EDC and FFE, as the results shown in Fig. 6(a). Two entropies with 1.4 and 1.5 bit/symbol are performed for PS-PAM-4 signals with the corresponding net rates of 105.2 Gb/s and 115.2 Gb/s, respectively, both above net 100 Gb/s. In the absence of a trans-impedance amplifier following the PD to boost the detected signal, approximately 2-dBm and 4-dBm ROPs are needed for net-105.2 Gb/s and net-115.2 Gb/s PS-PAM-4 signals, respectively. Namely, 10-Gb/s increase in net rate can be achieved at the price of a 2-dB penalty of ROP. Admittedly, the NGMI performance or net rate can be further improved using FIR-EDC and FFE with more number of taps to a certain extent. The NGMI performance without FIR-EDC is also presented for comparison in Fig. 6(a), showing the essential improvement of FIR-EDC. Besides, the eye-diagrams of 1.4- and 1.5-bit/symbol PS-PAM-4 signals with the performed FIR-EDC and FFE to combat 50-km accumulated CD at the maximal ROP of 7 dBm are shown in Figs. 6(b) and 6(d), respectively. Thanks to effective CD compensation, the eye-diagrams using FIR-EDC and FFE are much clearer than those only using FFE shown in Figs. 6(c) and 6(e).

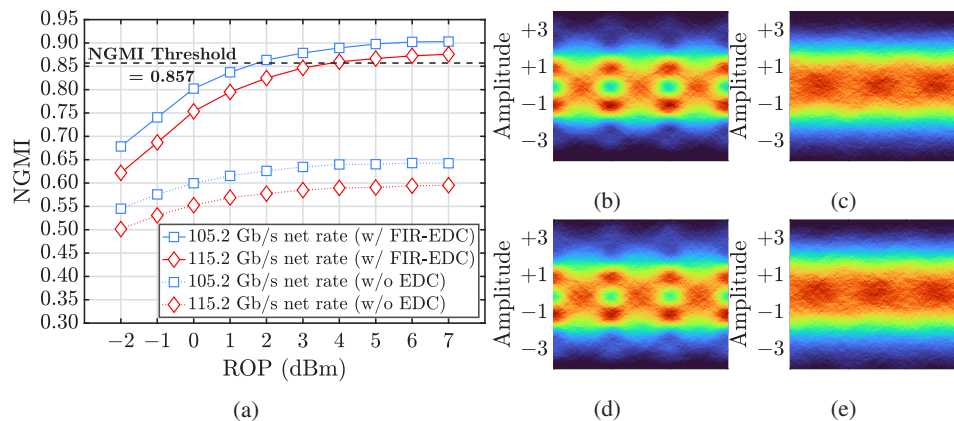


Fig. 6. (a) NGMI versus ROP for PS-PAM-4 signals at 105.2-Gb/s and 115.2-Gb/s net rates. Eye-diagrams of PS-PAM-4 signals at (b),(c) 105.2-Gb/s and (d),(e) 115.2-Gb/s net rates, with and without FIR-EDC, respectively.

4. Conclusion

In this paper, we have presented and evaluated a CD-aware PS-PAM-4 signal transmission scheme for C-band IM/DD system, in which a simple non-iterative FIR-EDC is successfully applied on rate-adaptable PS-PAM-4 signal at the transmitter to combat the CD-induced impairments. Applying only FFE at the receiver side, 100-Gbaud PS-PAM-4 signal transmission with FIR-EDC over 50-km SSMF has been realized, achieving 150-Gb/s line rate and 115.2-Gb/s net rate. Results also show the out-performance of the CD-aware PS-PAM-4 transmission scheme in achievable data rate compared with other benchmark schemes in high-speed IM/DD transmissions over 50-km SSMF. Specifically, a capacity improvement of 24.5% is obtained by the CD-aware PS-PAM-4 signal transmission scheme compared with FIR-EDC-based OOK signal transmission scheme, while further capacity improvement is achieved by the CD-aware PS-PAM-4 signal transmission scheme in comparison to the FIR-EDC-based PAM-4 signal transmission scheme or PS-PAM-4 signal transmission scheme without EDC. Therefore, the results indicate the practical feasibility of the proposal of FIR-EDC-based PS-PAM-4 signal transmission in beyond 100-Gb/s IM/DD transmissions over ER or beyond ER.

Funding. National Key Research and Development Program of China (2018YFB1801701); National Natural Science Foundation of China (62101602, 62035018); Project of the Shenzhen Municipal Science and Technology Innovation Commission (SGDX20201103095203030); Hong Kong Polytechnic University (G-SB1P); The Hong Kong Government General Research Fund (PolyU 15217620, PolyU 15220120); PolyU postdoc matching fund scheme of the Hong Kong Polytechnic University (1-W150).

Disclosures. The authors declare no conflicts of interest.

Data availability. Data underlying the results presented in this paper are not publicly available at this time but may be obtained from the authors upon reasonable request.

References

1. K. Zhong, X. Zhou, J. Huo, C. Yu, C. Lu, and A. P. T. Lau, "Digital Signal Processing for Short-Reach Optical Communications: A Review of Current Technologies and Future Trends," *J. Lightwave Technol.* **36**(2), 377–400 (2018).
2. T. Wettlin, S. Calabrò, T. Rahman, J. Wei, N. Stojanovic, and S. Pachnicke, "DSP for High-Speed Short-Reach IM/DD Systems Using PAM," *J. Lightwave Technol.* **38**(24), 6771–6778 (2020).
3. J. Zhang, X. Wu, Q. Yan, H. Tan, X. Hong, C. Fei, A. P. T. Lau, and C. Lu, "Nonlinearity-aware PS-PAM-16 transmission for C-band net-300-Gbit/s/λ short-reach optical interconnects with a single DAC," *Opt. Lett.* **47**(12), 3035–3038 (2022).
4. M. Gao, M. Liu, J. Ke, and B. Chen, "Probabilistically Shaped PAM-8 Transmission With Simplified Volterra Equalizer," *IEEE Photonics J.* **14**(6), 1–9 (2022).

5. X. Wu, J. Zhang, Q. Yan, A. P. T. Lau, and C. Lu, "C-band single-lane 290.4-Gb/s net rate PS-PAM-16 transmission over 1-km SSMF using low-complexity nonlinear equalization and single DAC," in *Conference on Lasers and Electro-Optics* (Optica Publishing Group, 2022), paper SM3J.6.
6. J. Zhang, M. Zhu, K. Wang, B. Hua, Y. Cai, M. Lei, Y. Zou, A. Li, W. Xu, J. Wang, X. Liu, Q. Zhou, and J. Yu, "Demonstration of Single-Lane 350-Gb/s PS-PAM-16 in the C-band using single-DAC for Data Center Interconnects," in *Optical Fiber Communication Conference* (Optica Publishing Group, 2021), paper Th5F.4.
7. M. S. Bin Hossain, G. Böcherer, T. Rahman, N. Stojanovic, P. Schulte, S. Calabrò, J. Wei, C. Bluemm, T. Wettlin, C. Xie, M. Kuschnerov, and S. Pachnicke, "Experimental Comparison of Cap and Cup Probabilistically Shaped PAM for O-Band IM/DD Transmission System," in *European Conference on Optical Communication* (2021), pp. 1–4.
8. J. Zhang, J. Yu, L. Zhao, K. Wang, J. Shi, X. Li, M. Kong, W. Zhou, X. Pan, B. Liu, X. Xin, L. Zhang, and Y. Zhang, "Demonstration of 260-Gb/s Single-Lane EML-Based PS-PAM-8 IM/DD for Datacenter Interconnects," in *Optical Fiber Communications Conference and Exhibition* (2019), pp. 1–3.
9. R. Rath, D. Clausen, S. Ohlendorf, S. Pachnicke, and W. Rosenkranz, "Tomlinson-Harashima Precoding For Dispersion Uncompensated PAM-4 Transmission With Direct-Detection," *J. Lightwave Technol.* **35**(18), 3909–3917 (2017).
10. J. Zhang, X. Wu, L. Sun, J. Liu, A. P. T. Lau, C. Guo, S. Yu, and C. Lu, "C-band 120-Gb/s PAM-4 transmission over 50-km SSMF with improved weighted decision-feedback equalizer," *Opt. Express* **29**(25), 41622–41633 (2021).
11. J. Zhang, H. Tan, X. Hong, J. Liu, C. Guo, C. Fei, X. Wu, A. P. T. Lau, S. Yu, and C. Lu, "Comparison of low-complexity sparse and weight-sharing nonlinear equalizers for C-band 100-Gbit/s DSB PAM-4 transmission over 60-km SSMF," *Opt. Express* **30**(20), 36343–36357 (2022).
12. H. Xin, K. Zhang, L. Li, H. He, and W. Hu, "50 Gbps PAM-4 Over Up to 80-km Transmission With C-Band DML Enabled by Post-Equalizer," *IEEE Photonics Technol. Lett.* **32**(11), 643–646 (2020).
13. J. Zhang, H. Tan, X. Hong, X. Wu, C. Fei, A. P. T. Lau, and C. Lu, "Improved Weighted Volterra DFE for C-Band 100-Gbit/s PAM-4 Transmission Over 60-km SSMF," *IEEE Photonics Technol. Lett.* **35**(4), 163–166 (2023).
14. H. Xin, K. Zhang, D. Kong, Q. Zhuge, Y. Fu, S. Jia, W. Hu, and H. Hu, "Nonlinear Tomlinson-Harashima precoding for direct-detected double sideband PAM-4 transmission without dispersion compensation," *Opt. Express* **27**(14), 19156–19167 (2019).
15. P. Zhu, Y. Yoshida, A. Kanno, and K. ichi Kitayama, "Analysis and Demonstration of Low-Complexity Joint Optical-Electrical Feedforward Equalization (OE-FFE) For Dispersion-Limited High-Speed IM/DD Transmission," *J. Lightwave Technol.* **41**(2), 477–488 (2023).
16. A. S. Karar, "Iterative Algorithm for Electronic Dispersion Compensation in IM/DD Systems," *J. Lightwave Technol.* **38**(4), 698–704 (2020).
17. X. Wu, A. S. Karar, K. Zhong, A. P. T. Lau, and C. Lu, "Experimental demonstration of pre-electronic dispersion compensation in IM/DD systems using an iterative algorithm," *Opt. Express* **29**(16), 24735–24749 (2021).
18. M. Yin, D. Zou, W. Wang, F. Li, and Z. Li, "Transmission of a 56 Gbit/s PAM4 signal with low-resolution DAC and pre-equalization only over 80 km fiber in C-band IM/DD systems for optical interconnects," *Opt. Lett.* **46**(22), 5615–5618 (2021).
19. D. Zou, F. Li, W. Wang, M. Yin, Q. Sui, and Z. Li, "Modified Gerchberg-Saxton Algorithm Based Electrical Dispersion Pre-Compensation for Intensity-modulation and Direct-detection Systems," *J. Lightwave Technol.* **40**(9), 2840–2849 (2022).
20. A. S. Karar, "Gerchberg-Saxton Based FIR Filter for Electronic Dispersion Compensation in IM/DD Transmission Part I: Theory and Simulation," *J. Lightwave Technol.* **41**(5), 1335–1345 (2023).
21. X. Wu, A. S. Karar, K. Zhong, Z. N. Gürkan, A. P. T. Lau, and C. Lu, "Gerchberg-Saxton Based FIR Filter for Electronic Dispersion Compensation in IM/DD Transmission Part II: Experimental Demonstration and Analysis," *J. Lightwave Technol.* **41**(5), 1428–1435 (2023).
22. A. Mahadevan, Y. Lefevre, W. Lanneer, P. Cautereels, D. van Veen, N. Kaneda, and V. Houtsma, "Impact of DFE on Soft-Input LDPC Decoding for 50G PON," in *Optical Fiber Communication Conference* (Optica Publishing Group, 2021), paper M3G.5.
23. H. Isono, "Latest standardization trend for next-gen high speed optical transceivers," in *Metro and Data Center Optical Networks and Short-Reach Links V*, vol. 12027 A. K. Srivastava, M. Glick, and Y. Akasaka, eds., International Society for Optics and Photonics (SPIE, 2022), p. 120270S.
24. H. Yamazaki, M. Nakamura, T. Kobayashi, M. Nagatani, H. Wakita, Y. Ogiso, H. Nosaka, T. Hashimoto, and Y. Miyamoto, "Net-400-Gbps PS-PAM transmission using integrated AMUX-MZM," *Opt. Express* **27**(18), 25544–25550 (2019).
25. D. Che and W. Shieh, "Squeezing out the last few bits from band-limited channels with entropy loading," *Opt. Express* **27**(7), 9321–9329 (2019).
26. T. Fehenberger, A. Alvarado, G. Böcherer, and N. Hanik, "On Probabilistic Shaping of Quadrature Amplitude Modulation for the Nonlinear Fiber Channel," *J. Lightwave Technol.* **34**(21), 5063–5073 (2016).
27. G. Böcherer, F. Steiner, and P. Schulte, "Bandwidth Efficient and Rate-Matched Low-Density Parity-Check Coded Modulation," *IEEE Trans. Commun.* **63**(12), 4651–4665 (2015).
28. L. Xue, L. Yi, W. Hu, R. Lin, and J. Chen, "Optics-Simplified DSP for 50 Gb/s PON Downstream Transmission using 10 Gb/s Optical Devices," *J. Lightwave Technol.* **38**(3), 583–589 (2020).

29. J. Zhang, H. Tan, L. Lu, L. Sun, X. Wu, A. P. T. Lau, and C. Lu, "Receive-diversity-aided power-fading compensation for C-band IM/DD OFDM systems," *Opt. Lett.* **48**(9), 2237–2240 (2023).
30. X. Wu, J. Zhang, A. P. T. Lau, and C. Lu, "Low-complexity absolute-term based nonlinear equalizer with weight sharing for C-band 85-GBaud OOK transmission over a 100-km SSMF," *Opt. Lett.* **47**(6), 1565–1568 (2022).
31. W. Cheng, M. Xiang, H. Yang, X. Huo, Y. Ma, J. Li, S. Fu, and Y. Qin, "C-band 100-GBaud/ λ PAM-4 transmission enabled by hardware-efficient nonlinear equalizer with weight-sharing pruning," *Opt. Lett.* **48**(2), 351–354 (2023).